Ice crystal classification based on silhouettes

H. Lindqvist*[,1], K. Muinonen[1,2], and T. Nousiainen[1]

[1]*Department of Physics, University of Helsinki, P.O. box 48, FI-00014 Finland.*
[2]*Finnish Geodetic Institute, P.O. Box 15, FI-02431 Masala, Finland.*

An automatic classification system for ice crystals is being developed based on shape parameters derived from crystal silhouette perimeters. As a test set, we use a small sample of crystal silhouettes captured by a cloud particle imager in cirrus clouds. Preliminary results show that the chosen parameters are suitable for separating single and aggregate crystals, and further, dividing these into plates, plate aggregates, single rosettes, and rosette aggregates. Columns and bullets remain as one unseparated group. The results are encouraging for future studies on larger observational data sets, but also offer a method for testing ice-crystal shape models against images of real ice crystals.

INTRODUCTION

Tropospheric cirrus clouds have a considerable effect on the radiation balance of the Earth. The radiative impact depends largely on the single-scattering properties of individual ice crystals, which in turn depend on the sizes and shapes, i.e. habits, of the crystals. This makes determining the habit distribution a critical factor for assessing ice-cloud radiative impacts. Since these clouds are found in 6-10 km height, observing single ice crystals is challenging and usually carried out using a cloud particle imager (CPI) attached to an airplane. CPI images reveal that large ice crystals possess shapes varying from single hexagonal columns, bullets, and plates to regular and irregular aggregates of these crystals [1]. The presence and proportion of each shape in an ice cloud depend on the prevailing meteorological conditions and, therefore, may vary between clouds. With an automatic classification system, the ice-crystal shape distribution of a cirrus cloud can be obtained efficiently. Classification also reveals valuable information on the ratio of cross-sectional area to the maximum dimension of the crystals: maximum dimension is used for defining crystal size; whereas, cross-sectional area determines the extinction cross section, a key parameter in radiative transfer considerations.

SILHOUETTE SHAPE CLASSIFICATION

CPI images of ice crystals present, in fact, silhouettes of crystals, as demonstrated in Fig. 1. They are taken by illuminating the crystal with a laser beam while the crystal is located in between the camera and the light source. Interpretation of silhouettes is challenging because three-dimensional shapes of real ice crystals cannot be unambiguously derived from CPI images without assumptions. For instance, single columns, bullets, and plates can produce exactly similar silhouettes when photographed directly from the top. Other complicating issues are the limited resolution and laser diffraction patterns on the images.

First step in the classification is to detach the perimeters of the crystals from the CPI images. Then, the extracted perimeters of crystals are discretized into 360 points using

*Corresponding author: Hannakaisa Lindqvist (hannakaisa.lindqvist@helsinki.fi)

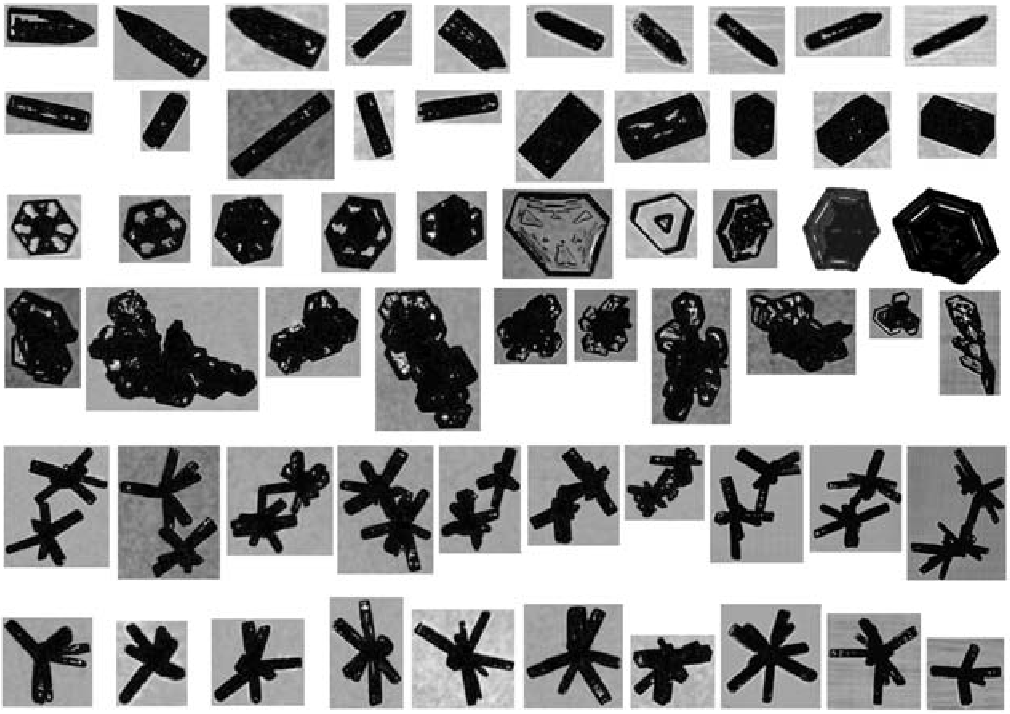

Figure 1. Sample ice crystal silhouettes. From top row to bottom: bullets, columns, plates, plate aggregates, column or bullet rosette aggregates, and column or bullet rosettes.

cubic splines so that the distance of two adjacent points along the perimeter is constant. The total length of the perimeter is then normalized to 360 degrees. This allows us to define an invariant angle γ, which corresponds to a certain proportion of the entire length of the perimeter, for instance $\gamma = 90$ degrees equals to 25 % of the total length of the perimeter. Angles are measured along the perimeter because this simplifies the treatment of non-starlike silhouettes.

In the next phase, certain shape parameters are calculated from the perimeter. The chosen parameters characterize the crystals in different ways and can be, therefore, useful in classification. The parameters considered are the following:

- Ratio A of the area inside the perimeter to the area of the convex hull.
- Aspect ratio. This is calculated as the ratio of the maximum length between two perimeter points to the maximum perpendicular width.
- Ratio R of the original length of the perimeter squared to the area inside the perimeter.
- Average of the length of the line segment $\bar{d}(\gamma)$ and its autocovariance $\mathrm{cov}(d(\gamma, \varphi))$ (cf. [2]): $d(\gamma)$ is the distance of two perimeter points separated by an invariant angle γ, $\bar{d}(\gamma)$ is the average over the perimeter, and $\mathrm{cov}(d(\gamma, \varphi))$ measures the correlation of two line segment lengths separated by an invariant angle φ. Here we have used $\gamma = 30$, 90, and 180 degrees, and $\varphi = 0$, 30, 90, and 180 degrees for the invariant angles, which results in 15 parameters.

- Average of the angle between the surface normal vectors $\bar{\alpha}(\gamma)$ and its autocovariance $\mathrm{cov}(\alpha(\gamma,\varphi))$: $\alpha(\gamma)$ is the angle measured between two surface normals of the perimeter points separated by γ. The invariant angles have values of $\gamma = 5$, 10, 30, 90, and 180 degrees, and $\varphi = 0$, 10, 30, 90, and 180 degrees, which leads to 30 parameters.

The classification itself includes two phases: first, we divide the crystals into compact and aggregate particles and then do the classification separately for both types. Compact and aggregate particles are separated according to parameter A, since it is equal or close to unity when considering compact crystal shapes, i.e. single plates, columns, or bullets. Thus, the value for compact particles is set to $A \geq 0.95$; other shapes are considered as aggregates.

In the second classification phase, we utilize different parameters for compact and aggregate crystals. Compact crystals are characterized by aspect ratio and parameter R; whereas for aggregates, we use A, aspect ratio, $\bar{d}$, $\mathrm{cov}(d)$, $\bar{\alpha}$, and $\mathrm{cov}(\alpha)$. Then, principal components analysis (PCA) is applied to the parameters to better distinguish the differences between the crystal properties. PCA transforms the input data vectors to a coordinate system where most of the information included in the input parameters is shown in fewer dimensions, defined by the most significant principal components. The outcome of PCA can then be used as a basis for classification.

PRELIMINARY RESULTS

As a test set we use altogether 60 CPI images, including both single and aggregated bullet, column, and plate crystals, 10 of each as shown in Fig. 1 on separate rows. The crystals in the images are identifiable and yet representative of their class, for instance the images of bullets and columns show varying aspect ratios and orientations.

The first results of the silhouette classification reveal that the division into compact and aggregate crystals based on the criterion $A \geq 0.95$ works perfectly for this test set, resulting in 30 compact and 30 aggregate crystals. For these separate groups, further results of the classification utilizing PCA are presented in Fig. 2, which shows the crystals in the coordinate system of the two most significant principal components of each data set. In the case of compact shapes, the plate-like crystals form a very dense group easy to identify; whereas, the bullets and columns tend to overlap. This means that the chosen parameters are not ideal for separating these two types of shapes. Also, some of the column-like crystals are close to the plates, which can be explained by looking at the test images: the columns with small aspect ratios do resemble the shape of the plate crystals in reality, as well.

The aggregate crystals divide into three distinguishable areas in the principal components space. According to Fig. 2, the single rosettes form a dense group indicating that the chosen parameters yield quite similar results to the rosettes, regardless of the observable differences among the silhouettes. This seems to apply to the rosette aggregates, as well. The plate aggregates, however, are distributed more widely. This can be due to the large variation in the number of the plates in the aggregates, which could be a useful feature in further classification and shape analyses.

CONCLUSION

The novel classification system for ice-crystal silhouettes proves to be efficient in separating the crystals of the test set: only single bullets and columns remain inseparable with the

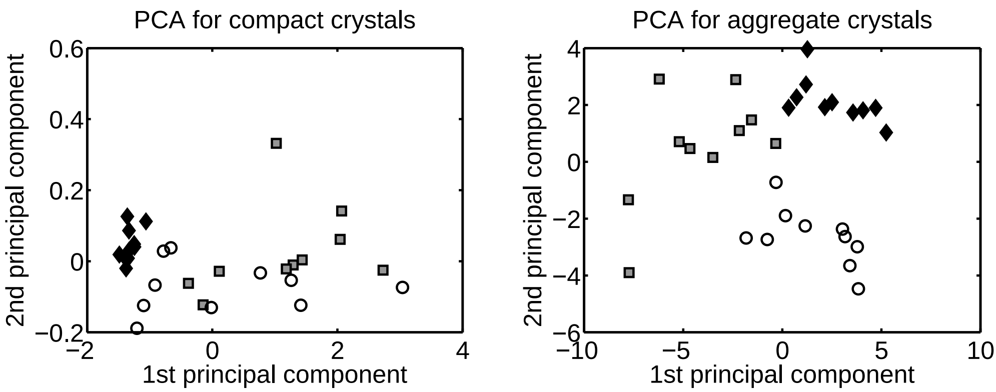

Figure 2. Compact (left) and aggregate (right) ice crystals in a coordinate system of two most significant principal components. For compact crystals, the squares, circles, and diamonds correspond to bullets, columns, and plates, and in the case of aggregate crystals, to plate aggregates, rosette aggregates, and single rosettes, respectively.

shape parameters used here. The next steps of the study are to develop new and improve the existing parameters used in PCA, and to apply an algorithm for classifying the PCA results automatically, for instance the nearest neighbor –algorithm. With this, the statistical reliability of the classification results can be assessed. Moreover, the classification needs to be tested for a larger data set that includes more irregularly shaped crystals. Applying the classification tool to the crystal silhouettes previously classified as irregulars or unclassifiable, can indeed reveal interesting common features among the crystals.

In addition to real CPI data, the classification system presented here can be applied to simulated crystal shapes. By generating synthetic silhouettes from model crystals and deriving the shape parameters it is possible to verify that model shapes statistically resemble the corresponding, real ice crystal shapes.

Finally, an intriguing and relevant question is that how do the single-scattering properties change between the classes and whether there is notable variation in the scattering characteristics inside a class. For this study, the models for ice crystals need to be improved to obtain a wider and more realistic view on the collection of shapes of naturally occurring ice crystals.

Acknowledgments: The authors wish to acknowledge Greg McFarquhar for providing the CPI data, Hanne Hakkarainen and Risto Makkonen for their contributions in ice-crystal image processing, and Antti Penttilä for advice in statistical matters. This work has been funded by the Academy of Finland (contracts 125180 and 127461).

REFERENCES

[1] J. Um and G. M. McFarquhar. Single-scattering properties of aggregates of plates. Q. J. R. Meteorol. Soc. **135** (2009).

[2] K. Muinonen. Inversion of small-particle silhouettes for Gaussian-sphere parameters. In: *9th Conference on Electromagnetic and Light Scattering by Nonspherical Particles: Theory, Measurements, and Applications*. N. Voshchinnikov (ed.) (2006).